

Inhibitors of human mitotic kinesin Eg5: Characterization of the 4-phenyl-tetrahydroisoquinoline lead series

Christine M. Tarby,* Robert F. Kaltenbach, III, Tram Huynh, Andrew Pudzianowski, Henry Shen, Marie Ortega-Nanos, Steven Sheriff, John A. Newitt, Patricia A. McDonnell, Neil Burford, Craig R. Fairchild, Wayne Vaccaro, Zhong Chen, Robert M. Borzilleri, Joseph Naglich, Louis J. Lombardo, Marco Gottardis, George L. Trainor and Deborah L. Roussell

Bristol-Myers Squibb Company, Route 206 and Province Line Road, Princeton, NJ 08543, USA

Received 14 December 2005; revised 13 January 2006; accepted 17 January 2006
Available online 3 February 2006

Abstract—In a high-throughput screening effort, a series of tetrahydroisoquinolines was identified as modest inhibitors of human Eg5. A medicinal chemistry optimization effort led to the identification of *R*-4-(3-hydroxyphenyl)-*N,N*-7,8-tetramethyl-3,4-dihydroisoquinoline-2(1*H*)-carboxamide (**32a**) as a potent inhibitor of human Eg5 (ATPase IC₅₀ 104 nM) with good anti-proliferative activity in A2780 cells (IC₅₀ 234 nM).

© 2006 Elsevier Ltd. All rights reserved.

Compounds that target mitosis (e.g., taxanes, vinca alkaloids)¹ have found clinical utility as chemotherapeutic agents. While effective against many cancer types, these agents can be compromised by acquired resistance and undesirable toxicities (neuropathy, neutropenia, and GI toxicity) linked to mechanism of action. As such, a need exists for small molecule agents which target mitosis by novel mechanisms as alternatives to the existing therapies.

Kinesins are a superfamily of motor proteins which hydrolyze ATP in order to transport cargo across microtubule networks. The microtubule associated kinesin Eg5 (also known as kinesin spindle protein (KSP)) is required for assembly and function of the mitotic spindle apparatus.² More specifically, Eg5 functions to bundle microtubules to form the bipolar mitotic spindle.^{2–4} Modulation of Eg5 activity, by immunodepletion of Eg5 protein or knockdown of Eg5 mRNA by siRNA, has been shown to cause aberrant mitotic spindle formation, cell cycle arrest in mitosis, and inhibition of proliferation of tumor cells in culture.^{4,5} Additionally,

treatment with reported human Eg5 inhibitors monastrol (**1**)⁶ and HR22C16 (**2a**)⁷ (Fig. 1) has been shown to induce cell death via apoptosis.⁸

Since agents which target Eg5 selectively would be expected to act only on cells undergoing cell division, we⁹ and others^{10,11} have undertaken efforts to identify small molecule inhibitors of this kinesin.

In a high-throughput screening effort, we identified a series of tetrahydroisoquinolines as inhibitors of human

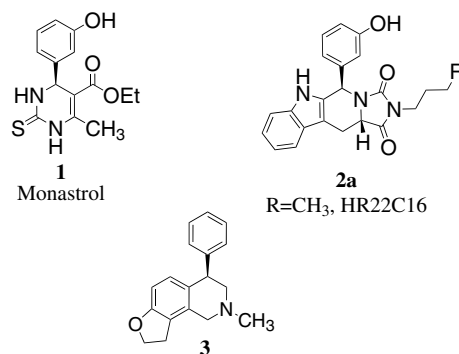


Figure 1. Eg5 inhibitors: Monastrol (**1**), HR22C16 (**2a**), and tetrahydroisoquinoline screening hit (**3**).

Keywords: Eg5 inhibitor; Kinesin inhibitor; Kinesin spindle protein; KSP; Eg5.

* Corresponding author. Tel.: +1 609 252 4669; fax: +1 609 252 7410; e-mail: christine.tarby@bms.com

Eg5. A representative member of the series, compound **3** (Fig. 1), displayed micromolar activity in both the Eg5 ATPase assay (IC_{50} 9.7 μ M)¹² and an anti-proliferation assay in A2780 ovarian carcinoma cells (IC_{50} 2.4 μ M).¹³ Thus, a medicinal chemistry program was initiated to further optimize the screening hit.

NMR experiments including $^1H/^{15}N$ chemical shift perturbation,¹⁴ saturation transfer difference (STD),¹⁵ and T_2 relaxation studies¹⁶ were performed on HTS compounds of interest to verify direct binding to Eg5. Competition experiments using STD with a known allosteric inhibitor demonstrated that compound **3** bound to the human Eg5 motor domain in an allosteric site previously described for other Eg5 inhibitors^{11,17} and not present in the *apo* structure of the enzyme. Guided by co-crystal structures of Monastrol¹⁷ (**1**) and HR22C16 analog (**2b**, R = NH₂),¹⁸ with the Eg5 motor domain, a binding model of compound **3** was constructed. The van der Waals affinity of the **2b** allosteric site for a methyl probe was mapped¹⁹ at a grid spacing of 0.5 Å. Compound **3** was docked to the site with the aid of this map, and the entire Eg5/ligand complex was allowed to relax through 1000 steps of energy minimization with the Tripos force field.²⁰ The resulting model and contour were used to guide SAR development (Fig. 2).

The tetrahydroisoquinoline (THIQ) scaffold was constructed from readily available starting materials using the synthetic route outlined in Scheme 1. Reductive amination of substituted benzaldehydes with ethanolamines gave the benzyl-substituted amino-alcohols **4**. Acid catalyzed cyclization of **4** with methanesulfonic acid in CH₂Cl₂ provided the THIQ core **5** in excellent yields. Alternatively, the cyclization precursor **4** could be obtained through NaBH₄-mediated reduction of the product from the alkylation of benzylamines and α -haloacetophenones. This latter sequence typically provided the THIQ core **5** in moderate yields.

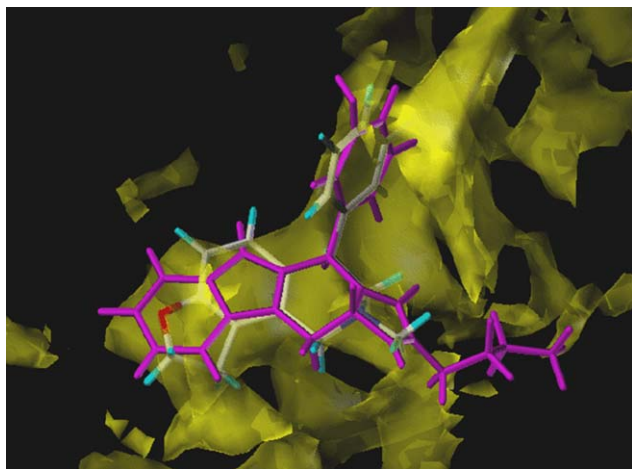
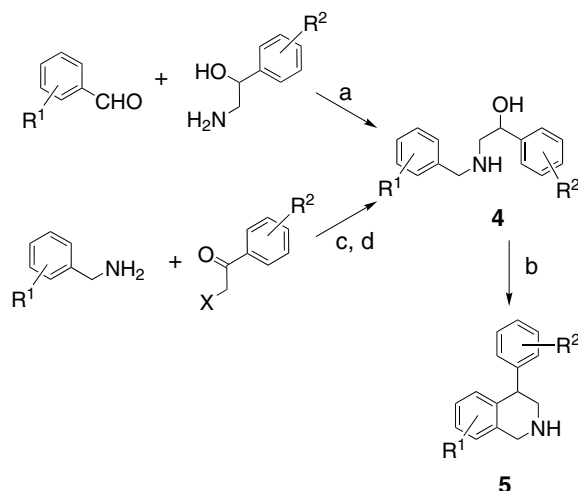
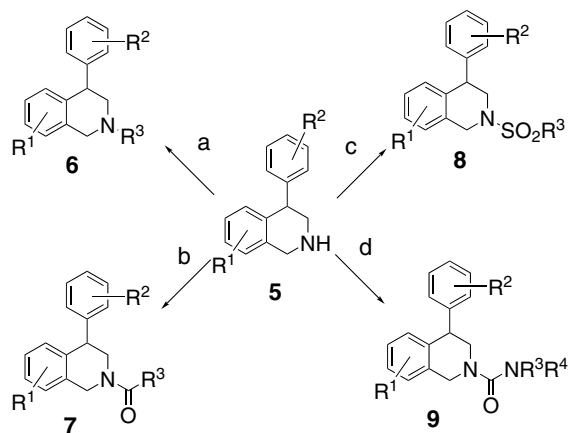


Figure 2. Compound **3** modeled into the human Eg5 motor domain:**2b** (magenta) crystal structure. MOL2MAP methyl probe affinity surface (van der Waals energy) is shown in yellow, contoured at -1.5 kcal/mol.



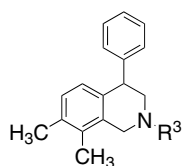
Scheme 1. Synthesis of the tetrahydroisoquinoline scaffold. Reagents and conditions: (a) NaBH₄, Et₃N, MeOH, 0–25 °C; (b) CH₃SO₃H, CH₂Cl₂, 0–25 °C; (c) 1 M K₂CO₃, EtOAc; (d) NaBH₄, MeOH, 0–25 °C.



Scheme 2. Reagents and conditions: (a) R³X, K₂CO₃, CH₃CN, 70 °C; (b) R³COCl, 1 M K₂CO₃, EtOAc or R³CO₂H, EDCI-HOBT, DMF; (c) R³SO₂Cl, 1 M K₂CO₃, EtOAc; (d) R³NCO or R³R⁴NCOCl, 1 M K₂CO₃, EtOAc.

Elaboration of the intermediate N-unsubstituted THIQ core is illustrated in Scheme 2. Alkylation with alkyl halides in the presence of potassium carbonate at 70 °C gave the N-alkyl analogs **6**. The acylated analogs **7** were prepared either by addition of an acid chloride to a two phase mixture of **5** in 1 M K₂CO₃/EtOAc (1:1) or through the coupling of the carboxylic acid with EDCI/HOBT. The sulfonated analogs **8** and the ureas **9** were prepared from the corresponding sulfonyl chlorides, isocyanates, or carbamoyl chlorides using standard procedures.

An initial scan of R¹ substitutions on the THIQ aryl ring yielded the 7,8-dimethyl groups as suitable replacements for the dihydrofuran ring of **3** (data not shown). Using the 7,8-dimethyl THIQ (**10**), the nitrogen substituent (R³) was optimized (Table 1). Incorporation of small alkyl groups on nitrogen provided compounds with

Table 1. 4-Phenyl-tetrahydroisoquinoline: optimization of the N-substituent

Compound	R ³	ATPase IC ₅₀ ^a (μM)	A2780 cytotoxicity IC ₅₀ ^a (μM)
10	–H	8.33	9.04
11	–CH ₃	18.4	7.30
12	–Et	25.2	5.30
13	– <i>i</i> Pr	11	6.28
14	–(CH ₂) ₂ Ph	>25	nd ^b
15	–(CH ₂) ₂ NH ₂	2.27	2.31
16	–(CH ₂) ₃ NH ₂	3.06	2.42
17	–(CH ₂) ₄ NH ₂	4.65	2.37
18	–(CH ₂) ₂ N-pyrrole	>25	nd
19	–(CH ₂) ₃ NMe ₂	8.88	3.24
20	–(CH ₂) ₄ NMe ₂	5.36	1.86
21	–COMe	17.9	nd
22	–COPh	16.4	7.77
23	–SO ₂ Me	>25	nd
24	–CO ₂ Me	14.4	nd
25	–CO ₂ Et	>25	nd
26	–CONH ₂	>25	nd
27	–CONHMe	>25	nd
28	–CON(Me) ₂	2.75	1.20
29	–CO-morpholine	22.3	nd
30	–CO-piperidine	12.8	2.83
31	–CON(Me)(CH ₂) ₃ NMe ₂	5.44	1.21

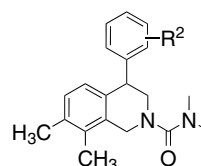
^a IC₅₀ values were derived from dose–response curves generated from triplicate data points.

^b nd, not determined.

modest activity in the human Eg5 ATPase assay (**11–13**), while use of larger N-alkyl substituents (>4C; e.g., **14**, **18**) led to loss of activity. However, when the N-alkyl chain contained a basic nitrogen 2–4 carbons away from the THIQ core (**15–17**, **19–20**), activity was retained or improved over the parent compound in both the ATPase and antiproliferation assays. From our computer model, we hypothesized that the charged side chain extended toward solvent.

Acylation of the THIQ nitrogen to provide amides, sulfonamides, carbamates or primary ureas afforded compounds with little to no activity. However, the *N,N*-dimethyl urea, **28**, was equipotent with the compounds containing a basic amine in the side chain (**15–17**). Larger disubstituted ureas (**29**, **30**) were less active than **28**. Combination of the disubstituted urea functionality with the basic amine containing side chain also provided micromolar compounds (e.g., **31**). Since we expected that compounds containing a basic nitrogen would have a greater potential for off-target activities, we chose to further explore SAR development in the *N,N*-dimethyl urea series (Table 2).

Our binding model of compound **3** with Eg5 indicated two carbonyls, from residues Trp127 and Glu118, were

Table 2. 4-Phenyl-tetrahydroisoquinoline: effect of substituents on the 4-phenyl ring

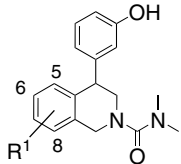
Compound	R ²	ATPase IC ₅₀ ^a (μM)	Cytotoxicity IC ₅₀ ^a (μM)
28	H	2.75	1.20
32	3-OH	0.306 (0.080)	0.376 (0.022)
33	4-OH	>25	nd ^b
34	3-CF ₃	13.2	nd
35	3-Cl	3.48	3.02

^a IC₅₀ values were derived from dose–response curves generated from triplicate data points. Values with standard deviations (in parentheses) are means of three independent experiments.

^b nd, not determined.

located in the pocket predicted to accommodate the 4-phenyl group. Both monastrol and HR22C16 analog **2a** donate a hydrogen bond through a phenol functionality to one of these moieties. Incorporation of a 3'-hydroxy group onto the 4-phenyl ring provided compound **32**, which exhibited a 7.7-fold increase in activity in the ATPase assay and 3-fold increase in anti-proliferative activity over **28** (Table 2). Moving the phenol substituent from the 3- to the 4-position (**33**) eliminated all detectable activity. Replacing the hydrogen-bond donating substituent with a 3-chloro or 3-trifluoromethyl provided compounds with micromolar activity.

With the 3'-hydroxy group incorporated, we turned our attention to optimization of the substituents on the THIQ aryl ring (R¹, Table 3). Initial SAR exploration of simple substituents at all four positions on the aryl ring quickly indicated a requirement for a substituent at the C7 or C8 position. The unsubstituted THIQ **36** and the C5 or C6 substituted compounds (data not shown) have IC₅₀s greater than 25 μM. Electron-withdrawing halogen groups incorporated at C7 provided compounds with modest to no activity in the ATPase assay (**37**, **38**), however, as the size of the C7 substituent increased and the electron-withdrawing capacity decreased, submicromolar activity was attained (**39**, **40**). Incorporation of both the 7-methyl and 7-methoxy compounds also provided compounds with potent submicromolar activities (**41**, **42**). At C8, halogens were not tolerated and substitution of a methyl (**46**) or methoxy (**48**) provided compound with micromolar activity. However, the 8-ethyl compound **47** exhibited equipotent activity to **32** in both assays. Substitution with groups at both the 7- and 8-positions provided mixed results. While 7,8-dimethyl compound **32** exhibited improved activity in the ATPase and antiproliferation assays over the singly substituted compounds (**41**, **46**), preparation of the 7,8-dimethoxy compound **49** resulted in substantial loss of activity over the singly substituted compounds (**42**, **48**). Submicromolar activities were observed for compounds with a ring appended in the

Table 3. 4-Phenyl-tetrahydroisoquinoline: effect of substitution on the tetrahydroisoquinoline aryl ring


Compound	R ¹	ATPase IC ₅₀ ^a (μM)	A2780 Cytotoxicity IC ₅₀ ^a (μM)
36	H	>25	nd
37	7-F	>25	nd ^b
38	7-Cl	2.49	1.19
39	7-Br	0.808 (0.089)	0.879 (0.143)
40	7-I	0.317 (0.080)	0.363 (0.015)
41	7-Me	0.595	0.851
42	7-OMe	0.617 (0.019)	0.402 (0.032)
43	8-F	>25	nd
44	8-Cl	>25	nd
45	8-Br	>25	nd
46	8-Me	4.71	2.05
47	8-Et	0.344	0.186
48	8-OMe	1.78	0.332
32	7,8-Me ₂	0.306 (0.080)	0.376 (0.022)
49	7,8-(OMe) ₂	12.8	2.92
50	7,8-Cl ₂	1.27	3.44
51	7,8-naphthyl	0.477	0.373
52	7,8-(–(CH ₂) ₂ O–)	0.639	0.235

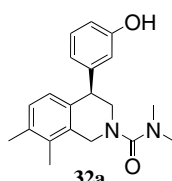
^a IC₅₀ values were derived from dose–response curves generated from triplicate data points. Values with standard deviations (in parentheses) are means of three independent experiments.

^b nd, not determined.

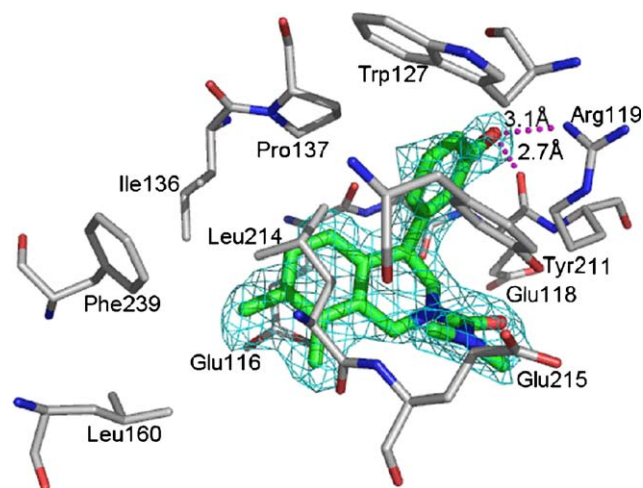
7,8-position (**51**, **52**). In general, close correlation between the data obtained in the ATPase and cell proliferation experiments was observed across all program compounds.

Compound **32** was resolved into its enantiomers and the active enantiomer **32a** (Fig. 3, *R*-isomer²¹) was used for co-crystallography experiments and further biological evaluation.

The X-ray crystal structure of **32a** in complex with Mg²⁺ and ADP was determined to 2.3 Å resolution.²² As predicted from our modeling studies, compound **32a** binds in the known allosteric pocket of Eg5.^{9,17} This allosteric binding site of **32a** is approximately 13 Å from the nucleotide binding site and causes rearrangement of backbone and side chains relative to the Mg-ADP struc-



32a
ATPase IC₅₀ 0.104 (0.044) μM
A2780 Cytotoxicity IC₅₀ 0.234 (0.036) μM

Figure 3. Compound **32a**.**Figure 4.** The binding site for compound **32a** on human Eg5. The compound is shown with thick rods and the protein is shown with thinner rods. The initial 2F_o – F_c electron density map contoured at 1σ is shown in cyan mesh. Figure created using PyMol.²⁴

ture of the protein.²³ The binding site for compound **32a** is shown in Figure 4. The phenol moiety of compound **32a** binds in a hydrophobic sub-pocket surrounded by side chains of Arg 119, Trp 127, Ala 133, Pro 137, Tyr 211, and Leu 214 with additional van der Waals interactions contributed by the main chain of Gly 117 and Glu 118, and the side chain of Asp 130. Additionally, the phenol forms hydrogen bonds to the Glu 118 carbonyl oxygen and the Arg 119 side chain. The 7,8-dimethyl substituted aryl ring of the THIQ is sandwiched between the side chains of Glu 116 and Leu 214 with additional van der Waals interactions with the side chains of Ile 136, Pro 137, Leu 160, Ala 218, and Phe 239, and the main chain of Glu 116. The piperidine moiety of the THIQ forms van der Waals contacts with the side chain of Ala 218 and the carbonyl oxygens of Glu 116 and Gly 117. The dimethyl urea moiety, which is pointed out of the binding pocket, forms van der Waals contacts with both the main and side chains of Leu 214 and Glu 215, and the side chains of Tyr 211, Arg 119, and Ala 218.

Development of structure activity relationships during optimization of the THIQ series of Eg5 inhibitors demonstrated a correlation between the microtubule-dependent Human Eg5 ATPase activity and A2780 ovarian carcinoma cell proliferation. In order to confirm that the cytotoxicity displayed by the THIQ series was a consequence of Eg5 inhibition, we further characterized the cellular activity of compound **32a**.

Cells with reduced Eg5 activity, for example by immunodepletion or small molecule inhibitors, display a characteristic mitotic cell phenotype and arrest in mitosis.^{4,6} As shown in the confocal fluorescent microscopy images of Figure 5, compound **32a** induced the formation of monopolar mitotic spindles in kangaroo rat kidney epithelial cells (PtK2) after 4 h treatment.²⁵ Multiple monopolar mitotic spindles but no bipolar mitotic spindles were observed (Fig. 5A). Under higher magnifi-

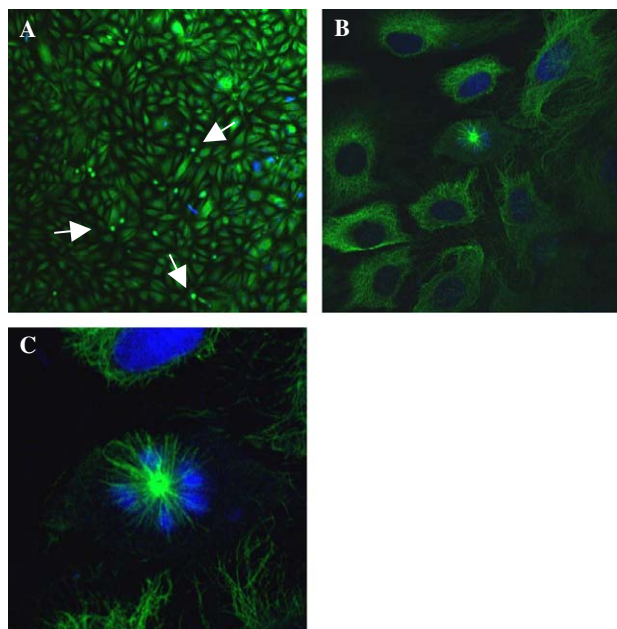


Figure 5. Confocal fluorescent microscopy images of PtK2 following treatment with 8.6 μM compound **32a** for 4 h. Monopolar mitotic spindles (arrowheads) in a representative field of cells at increasing magnification (10 \times , 63 \times , and 63 \times Zoom in panels A, B, and C, respectively), microtubules (green), and chromosomal DNA (blue).

cation (Fig. 5C), several DAPI-stained chromosomes (blue) are detected in the focal plane with microtubules of the mitotic spindle (green).

Compound **32a** also arrested cells in mitosis. A2780 ovarian carcinoma cells treated with compound **32a** for 17 h, corresponding to approximately one cell cycle, showed an increase in the mitotic index (percentage of cells in M phase) relative to untreated cells, as quantified by flow cytometry.¹³ The induction of mitotic arrest at 17 h is in agreement with the cytotoxicity observed in A2780 cells at 72 h (Table 4). Further evaluation of the cytotoxic activity of compound **32a** revealed anti-proliferative activity against multiple tumor cell lines (breast, colorectal, lung, ovarian, and prostate). Cytotoxicity IC_{50} values in the different cell lines varied less than 0.6 log of the mean, as graphically depicted in the mean bar graph (Fig. 6). As expected for an inhibitor of the essential protein Eg5, compound **32a** was equipotent in all cell lines tested, including both A2780S

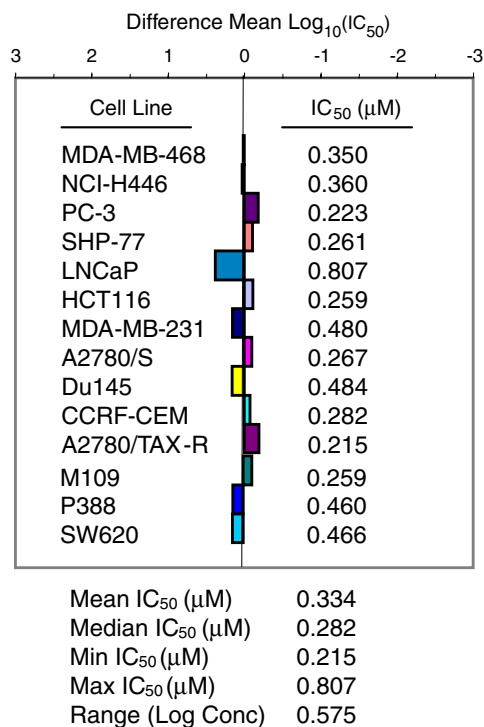


Figure 6. Compound **32a** Eg5 inhibitor **32a** demonstrated cytotoxic activity against a panel of tumor cell lines.²⁷ IC_{50} s were determined after 72 h exposure. The mean bar graph depicts the difference between the log of individual cell line IC_{50} values relative to the mean log of all the IC_{50} values. Relative sensitivities are shown; right-projecting bars are more sensitive cell lines and left-projecting bars are less sensitive cell lines.

taxol-sensitive (IC_{50} 0.267 μM) and A2780-TAXR taxol-resistant (IC_{50} 0.215 μM) cell lines.²⁶

Modeling-guided optimization of the tetrahydroisoquinoline screening hit **3** led to the identification of compound **32a**, a sub-micromolar human Eg5 inhibitor. Biological characterization demonstrated that compound **32a** displays cellular activities in secondary assays consistent with an Eg5 mechanism of action. Compounds from the tetrahydroisoquinoline series are novel human Eg5 inhibitors with promising preclinical activity profiles and represent significant new leads for further optimization.

Table 4. Cell cycle analysis

Compound	Concentration (μM)	A2780 cell cycle profile			Mitotic index
		% G1 Phase	% S Phase	% G2 + M Phase	% M Phase
32a	0.257 ^a	9.1	11.8	73.2	39.3
32a	0.328 ^b	3.1	5.9	84	52.2
DMSO	0.08% ^c	41.4	37.5	14.8	3.2
Nocodazole	0.1 ^d	12	15.7	62.1	23.7

Experimental details described in Ref. 13.

^a A2780 IC_{50} .

^b A2780 IC_{90} .

^c neg. control.

^d pos. control.

Acknowledgments

The authors acknowledge Luciano Mueller for his assistance with the NMR experiments; Timothy Spicer and Jonathan O'Connell for high-throughput screening experiments; Gretchen Schroeder for her assistance examining the HTS data; Atsu Apedo for the CD–UV spectrum of compound **32a**; Rolf Rysek for cloning Eg5 DNA sequence; Gerald Duke for the preparation of Eg5 protein used in the Eg5 enzymatic assays; Russell Peterson and Kathy Johnston for cell panel cytotoxicity studies; Anne Lewin for the confocal microscopy images; and Mike Poss for program discussions around the lead series.

References and notes

- Dutcher, J. P.; Novik, Y.; O'Boyle, K.; Marcoullis, G.; Secco, C., et al. *J. Clin. Pharmacol.* **2000**, *40*, 1079.
- Sawin, K. E.; LeGuellec, K.; Philippe, M.; Mitchison, T. J. *Nature* **1992**, *359*, 540.
- Walczak, C. E.; Vernos, I.; Mitchison, T. J.; Karsenti, E.; Heald, R. *Curr. Biol.* **1998**, *8*, 903.
- Blangy, A.; Lane, H. A.; d'Herin, P.; Harper, M.; Kress, M., et al. *Cell* **1995**, *83*, 1159.
- Weil, D.; Garcon, L.; Harper, M.; Dumenil, D.; Dautry, F., et al. *Biotechniques* **2002**, *33*, 1244.
- Mayer, T. U.; Kapoor, T. M.; Haggarty, S. J.; King, R. W.; Schreiber, S. L., et al. *Science* **1999**, *286*, 971.
- Hotha, S.; Yarrow, J. C.; Yang, J. G.; Garrett, S.; Renduchintala, K. V.; Mayer, T. U.; Kapoor, T. M. *Angew. Chem. Int. Ed. Engl.* **2003**, *42*, 2379.
- (a) Marcus, A. I.; Peters, U.; Thomas, S. L.; Garrett, S.; Zelnak, A., et al. *J. Biol. Chem.* **2005**, *280*, 11569; (b) Leizerman, I.; Avunie-Masala, R.; Elkabets, M.; Fich, A.; Gheber, L. *Cell Mol. Life Sci.* **2004**, *61*, 2060.
- Kim, K. et al. (Manuscript in preparation).
- (a) Sakowicz, R.; Finer, J. T.; Beraud, C.; Crompton, A.; Lewis, E., et al. *Cancer Res.* **2004**, *64*, 3276; (b) Sunder-Plassmann, N.; Sarli, V.; Gartner, M.; Utz, M.; Seiler, J., et al. *Bioorg. Med. Chem.* **2005**, *13*, 6094; (c) Bergnes, G.; Brejc, K.; Belmont, L. *Curr. Top. Med. Chem.* **2005**, *5*, 127.
- Cox, C. D.; Breslin, M. J.; Mariano, B. J.; Coleman, P. J.; Buser, C. A., et al. *Bioorg. Med. Chem. Lett.* **2005**, *15*, 2041.
- Burford, N. et al. ATPase assays with Eg5 motor domain protein were performed with Kinase Glo Kit as described by the manufacturer (Promega) (Manuscript in preparation).
- Human tumor cell line maintenance and cell-based assays were performed as described in (a) Kim, K. S.; Kimball, S. D.; Misra, R. N.; Rawlins, D. B.; Hunt, J. T., et al. *J. Med. Chem.* **2002**, *45*, 3905(b) Rouscell, D. et al. (Manuscript in preparation).
- Shuker, S. B.; Hajduk, P. J.; Meadows, R. P.; Fesik, S. W. *Science* **1996**, *274*, 1531.
- Mayer, M.; Meyer, B. *Angew. Chem. Int. Ed.* **1999**, *38*, 1784.
- Navon, G.; Lanier, A. *J. Magn. Reson.* **1972**, *8*, 14.
- Yan, Y. S. V.; Xu, B.; Homnick, C.; Halczenko, W.; Buser, C. A.; Schaber, M.; Hartman, G. D.; Huber, H. E.; Kuo, L. C. *J. Mol. Biol.* **2004**, *335*, 547.
- Newitt, J. Sheriff, S. Unpublished results.
- Goodford, P. J. *J. Med. Chem.* **1985**, *28*, 849.
- Clark, M. C. R. D., III; Van Opdenbosch, N. *J. Comp. Chem.* **1989**, *10*, 982.
- R-configuration determined through CD–UV and computational experiments. Structural assignments subsequently confirmed by co-crystallography in Eg5 binding pocket.
- (a) PDB Deposition number is **2FME**.; (b) Newitt, J. et al. (Manuscript in preparation).
- Turner, J.; Anderson, R.; Guo, J.; Beraud, C.; Fletterick, R., et al. *J. Biol. Chem.* **2001**, *276*, 25496.
- DeLano, W. L. The PyMol Molecular graphics System (2002). DeLano Scientific, San Carlos, CA, USA. <http://www.pymol.org>.
- PtK2 cells were grown in minimal essential medium (MEM) supplemented with 10% fetal calf serum in an incubator at 37 °C, 5% CO₂. Cells were plated onto chamber slides at a density of 10,000 cells/cm². Treatment was initiated 24 h after plating with the addition of compound. After 4 h of treatment, compound was removed, methanol was added for 2 min to fix and permeabilize cells, and 3% bovine serum albumin (BSA) in phosphate-buffered saline (PBS) was added to block. DNA was stained with 50 nM DAPI and microtubules were stained with Monoclonal Anti-tubulin (Sigma) followed by FITC-conjugated goat anti-mouse (ICN/Cappell Fluorescein conjugate F(AB')₂FRAGMENT to Mouse IGG whole molecule).
- Giannakakou, P.; Sackett, D. L.; Kang, Y. K.; Zhan, Z.; Buters, J. T., et al. *J. Biol. Chem.* **1997**, *272*, 17118.
- (a) MDA-MB-468: Human breast carcinoma; NCI-H446: Human small cell lung carcinoma; PC-3: Human prostate carcinoma; SHP-77: Human small cell lung carcinoma; LNCaP: Human prostate carcinoma; HCT-116: Human colon carcinoma; MDA-MB-231: Human breast carcinoma; A2780S: Human ovarian carcinoma, taxol sensitive; Du145: Human prostate carcinoma; CCRF-CEM: Human leukemia; A2780/TAX-R: Human ovarian carcinoma, taxol resistant; M109: Murine lung carcinoma; P388: Murine leukemia; SW620: Human colorectal carcinoma; (b) Lee, F. Y. F.; Borzilleri, R.; Fairchild, C.; Kim, S. H.; Long, B. H.; Raventos-Suarez, C.; Vite, G. D.; Rose, W. C.; Kramer, R. A. *Clin. Cancer Res.* **2001**, *7*, 1429.